DOI: 10.15480/882.9370

Eighth International Symposium on Marine Propulsors
smp'24, Berlin, Germany, March 2024

Ship-Scale CFD Self-Propulsion validation – SMP'2024 vs SMP'2015

Dmitry Ponkratov[1], Miles Wheeler[2]

[1]Siemens Digital Industries Software, London, UK
[2]Siemens Digital Industries Software, Bellevue, WA USA

ABSTRACT

At SMP'2015 the author published a paper about ship-scale CFD self-propulsion validation for a tanker. The paper proposed at SMP'2024 outlines the significant development of the same subject over nearly ten years. The importance of the challenge for the industry led to obtaining comprehensive publicly available ship-scale validation cases. One of these cases is the JoRes1 tanker (which has similar dimensions to the MR tanker reported in 2015) considered within the global JoRes Joint Research Project. The details of the ship scale measurement are featured in this paper. The project participants ran this case blindly not knowing the sea trial results (propeller revolutions and power) as only the geometry and vessel speeds were provided. The presented CFD results are obtained by a single participant (Siemens Digital Industries software) showing a good comparison with the ship scale measurements.

Keywords

JoRes1 tanker, CFD, Ship scale, Propeller flow, Validation.

1 INTRODUCTION

In July 2023 the International Maritime Organization adopted a new strategy aiming to reduce Greenhouse Gas emissions from the global shipping to zero by or around 2050 (IMO 2023). In September 2023 DNV released the 2050 forecast (DNV 2023) showing that the initial and important stage of the zero-emission challenge relies on the ship's energy efficiency. The digitalization of the global maritime industry should help to address this objective. Computational Fluid Dynamics (CFD) has been actively used for ship design for a few decades, however, in the past, the main focus was aimed at model scale simulations. There were two main reasons for that: 1. The computational power of computers did not allow practitioners to build a mesh that was able to accurately calculate a ship scale case within an acceptable time for practical engineering tasks. 2. The validation cases were mainly available in model scale (KCS, KVLCC2 etc).

The development in computational power has successfully addressed the first challenge, and pioneering ship-scale validated calculations appeared in the industry about 10 years ago (Ponkratov and Zegos 2014, Ponkratov and Zegos 2015) and presented at the SMP'2015 symposium. Nevertheless, these works had a few challenges. For the MR tanker case used for the validation, the hull roughness measurements were not performed. Moreover, the sea trials were not post-processed according to the ISO15016 standard and only integral characteristics (rpm, torque and thrust) were measured and compared. In addition to that the authors knew the sea trials results when they performed CFD calculations, so it was not a blind validation exercise.

The second challenge of publicly available ship-scale validation cases was not addressed for a long time until Lloyd's Register (LR) organized the first workshop on ship-scale computer simulations (Ponkratov 2017). However, the MV "Regal", introduced at the LR CFD workshop, also did not have hull and propeller roughness measurements. The participants of that workshop were asked to simulate the roughness according to their internal working procedures and make necessary assumptions. As a result, it introduces some uncertainties.

In the impressive master theses by Mikkelsen and Steffensen (2016) the validation was performed against four sets of sisterships' sea trials. Nevertheless, the authors outlined the uncertainties related to the fact that the simulations have been performed with the stock propeller instead of the actual propeller (the propeller designer did not permit to use of the actual propeller geometry) and the fact that air resistance, bilge keel resistance and hull roughness resistance were calculated using the ITTC procedure instead of being modelled in CFD.

Niklas and Pruszko (2019) performed CFD validations for the "Nawigator XXI" research and training vessel. It is a very detailed and deep work; however, the authors did not discuss the uncertainty related to the propeller pitch angles. It is usually quite difficult to ensure the correct pitch angle position at the trials. Moreover, it is understood the hull roughness was also not measured before the trials, so the authors assumed the equivalent sand grain roughness, Ks, to be equal to 150 μm.

Sun et al (2020) performed CFD ship scale validation based on sea trials results for 9 bulk carriers with the same hull form, propeller, and rudder. As the roughness effect was not the focus of their article, they used the Bowden–Davison empirical formula to avoid introducing more complicated uncertainty sources to CFD simulation. It is understood they used a Ks value of 90 μm.

Orych et al (2021) considered for their validation study a set of sea trials for 12 single screw vessels. They assumed

the Average Hull Roughness (AHR) to be 100 μm. With the employed Aupoix-Colebrook roughness model (AHR/Ks = 5) it gives the equivalent sand grain roughness Ks value of 20 μm. The propeller roughness was assumed to be 30 μm.

Mikulec and Piehl (2023) performed ship-scale CFD validation on a 34m Research Vessel "Gunnerus". The assumed equivalent sand-grain roughness Ks value was 30 μm. Unfortunately, this vessel is equipped with two azimuth thrusters, so there was a challenge with measurements of propeller power as strain gauges could not be installed inside the housing.

As it can be seen, various assumptions can be made about the hull roughness and other parameters and these assumptions can significantly affect the CFD results. The main challenge is associated with the fact that sea trials procedures (like ISO15016) were not developed for the purposes of CFD validation. The main objective of these procedures is to confirm contractual speed. As a result, these procedures do not require hull and propeller roughness measurements (which are important for CFD) and still rely on simplified methods (sea state assessment by the naked eye, visual observations of vessel draughts etc). Clearly to develop an accurate case for CFD validation stricter requirements for the ship scale measurements should be implemented.

These expectations led to organizing and executing a JoRes joint research project aiming to develop an industry-recognized benchmark for ship-scale CFD validation. As discussed in Ponkratov (2023) 6 vessels were considered within the project. For all of them, comprehensive ship scale measurements were performed including actual hull and propeller roughness checks. For one of the vessels (JoRes1 tanker) ship scale PIV measurements of the propeller flow were also performed.

It should be also noted that the sea trials for this vessel were performed at the loaded draught which makes these measurements very unusual. After the trials, model tests were conducted at SSPA/RISE and HSVA for the conditions identical to the trials.

2 JORES1 TANKER SHIP SCALE MEASUREMENTS

The following activities took place before the actual trials: the hull and propeller roughness measurements were performed in the dry dock, strain gauges were installed on the propeller shaft to measure propeller torque, the optical sensor was installed next to the shaft to measure propeller shaft speed, anemometers were installed on the antenna mast to get wind characteristics, etc. Most importantly the FlowPike - a specially developed unit for ship scale PIV (Particle Image Velocimetry) measurements was installed (Ponkratov et al. 2022).

The Average Hull Roughness (AHR) of the hull was measured in the dry dock and the value was 218 μm. It should be noted that the recent investigations (Schultz and Hutchins 2021) proposed a novel method of hull roughness conversion. The previous methods were based on arithmetic averaging of roughness measurement along

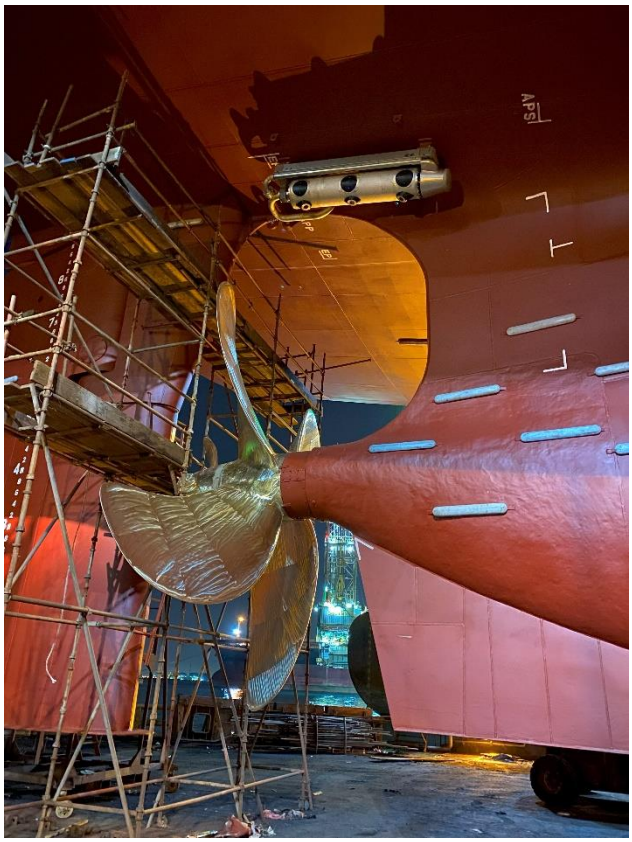

Figure 1: FlowPike on the JoRes1 tanker in the dry dock.

the hull. Nevertheless, it is clear the contribution of roughness on the ship bow and ship stern is very different.

Hutchins et al (2023) suggested the power mean method which was implemented for the JoRes tanker case. So, the AHR for the hull of 218 μm gives the sand grain roughness equivalent Ks of 53 μm.

The propeller roughness was measured and estimated to be 4 μm. All the detailed reports showing the measurement values and postprocessing details will be publicly available within the JoRes project benchmark in 2024.

The sea trials were conducted according to the ISO15016:2015 standard. Before the trials, the vessel was stopped at sea to deploy the wave buoy, record vessel draughts and measure water properties. Later on, after the trials, the vessel was stopped again to record vessel draughts and measure water properties. The trials were performed at four shaft speeds (60, 75, 90 and 96 RPM). Normally, the ISO standard requires conducting 2 runs for each RPM setting (minimum of 10 min each), however, as it was expected that 10 min would not be enough for sufficient PIV measurements, the decision was made to make the duration of each run 40 min. Moreover, for 75 and 90 RPM settings, 4 runs were performed, resulting in a total of 12 performed runs.

The main part of the PIV measurements was done at two speeds (75 and 90 RPM). Additionally, PIV measurements were done at a third speed (96 RPM), where a limited program could be executed. Each run consisted of measuring at different rotation angles of the FlowPike for

either 80 s or 120 s; this amounted to either 800 or 1200 images per one angle. The device was rotated to cover a total sector of either 70 or 140 degrees (the first of the double runs had a 70-degree sweep, the second a 140-degree sweep), which is a large part of the wake. The centre of each sweep was pointed at the expected position of the wake peak. Repeat measurements were also performed systematically; in fact, most angles were measured twice within one run, which will result in better statistics and will enable us to investigate that there are no large-scale flow effects that could bias the measurements. All the details of the PIV setup are reported in Birvalski et al. (2023).

Overall, the quality of the PIV images was very good, comparable to what was achieved with the FlowPike in the model basin previously. The concentration of the seeding particles was somewhat lower than ideal, but this will not have a large influence on the resulting quality. Likewise, the PIV inter-frame time needed to be kept low due to the high flow velocity through the laser sheet, but the resulting particle displacement is considered sufficiently high for a good dynamic range. In total 6.5 terabytes of PIV data were recorded.

Despite all the effort to perform sea trials as accurately as possible it is practically impossible to achieve zero uncertainty. As discussed in Ponkratov and Strujik (2023) the sea trials uncertainty level for this case was 4-6%.

3 JORES1 TANKER SHIP CFD MODEL

In addition to performing sea trial measurements, the JoRes project sought to see how well CFD models can blindly predict these full-scale sea trial measurements. About 20 project participants contributed to the CFD study: only geometries, initial draught conditions, and speeds (13.34 knots and 11.25 knots) were shared. They were asked to calculate the case and provide the workshop organizers with torque, rpm, power, and flow data at a specified section. (identical to the PIV plane on the actual vessel) The results presented in this paper were calculated by one participant (Siemens Digital Industries Software).

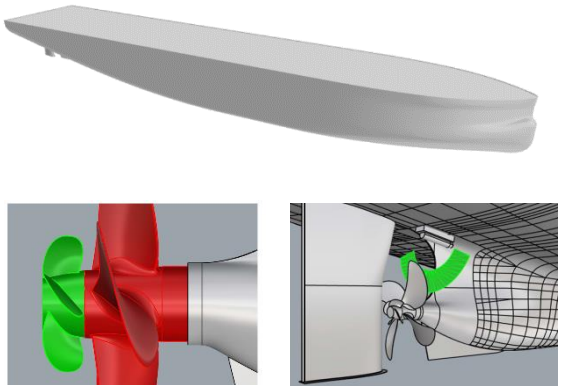

Figure 2: JoRes Tanker 1 geometry (top). The propulsor includes an FPP propeller and a PCBF energy-saving device (lower left). The Flow Pike measures the average flow field highlighted with the green area (lower right).

As this was a blind CFD benchmark, no extensive verification or validation procedures were performed, but moreover, best practices established from experience and insight from the JoRes community were used to generate the model. Part of the JoRes project, which is outside the scope of this paper, consisted of several investigations by the participants to develop best practices in terms of both mesh and time discretization. Extensive verification and validation studies were explored on a 150 m long cargo ship, the MV Regal, under self-propulsion and validated against sea trial experiments as well. The findings produced a deviation amongst participants on the order of 2% and results were deemed validated against sea trial measurement. These findings gave the participants confidence in their simulation approaches, and the practices generated in the cargo ship investigations were directly applied to this tanker ship for the blind benchmark study.

Siemens Simcenter STAR-CCM+ version 2202 was used in this study. The computational model uses a finite volume-based approach using a segregated solver for incompressible fluids. The SIMPLE (Semi-Implict Pressure Linked Equations) algorithm was used to couple the velocity and pressure fields. A 2nd order convection scheme was used, and AMG solver convergence tolerances were set to 0.01. A pseudo-transient approach was used with varying time steps using a 1st order time discretization. The free surface was modelled with a Volume of Fluid (VOF) solver and a high-resolution interface capturing (HRIC) scheme with an angle factor of 0.15. The governing equations relating continuity, momentum, and VOF are described in Equations 1-3 below.

$$\frac{\partial \rho}{\partial t} + \frac{\partial (\rho u_j)}{\partial x_j} = 0 \quad (1)$$

$$\frac{\partial (\rho u_i)}{\partial t} + \frac{\partial (\rho u_i u_j)}{\partial x_j} = -\frac{\partial p}{\partial x_i} + \frac{\partial}{\partial x_j}\left[\mu\left(\frac{\partial u_i}{\partial x_j} + \frac{\partial u_j}{\partial x_i} - \frac{2}{3}\delta_{ij}\frac{\partial u_k}{\partial x_k}\right)\right] + \rho f_i \quad (2)$$

$$\frac{\partial B}{\partial t} + \frac{\partial (B u_i)}{\partial x_i} = 0 \quad (3)$$

Where u is the flow velocity, ρ is the mixture density, t is time, f is the body force, and B represents the volume fraction occupied by air, so that the effective fluid density ρ and viscosity μ are calculated as

$\rho = \rho_{air} B + \rho_{water}(1 - B)$

and $\mu = \mu_{air} B + \mu_{water}(1 - B)$.

Turbulence was modeled using a RANS (Reynolds Averaged Navier Stokes) formulation using the K-Omega SST turbulence model.

The computational domain and mesh refinements were built in the same manner outlined by Wheeler in his paper on parametric template creation for smooth hulls (2021), with some modifications made to account for appendages,

roughness, and the geometrically modelled propeller. This study used a refinement ratio of 50. In other words, the base size of the mesh was set to L / 50, where L is the length of the vessel, and all meshing parameters are defined based on this value. Images of the computational mesh are shown in Figure 3.

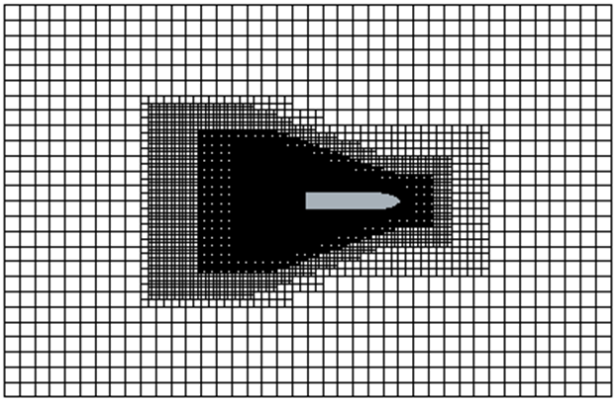

(a) Computational Mesh at Z = 0

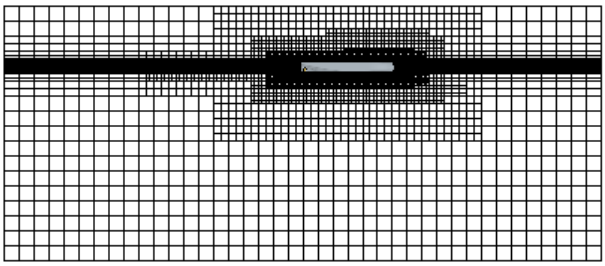

(b) Computational Mesh at Y=0

Figure 3: Images of the computational domain and mesh from (a) top view and (b) side view.

As previously mentioned, hull roughness was simulated using the procedure described by Hutchins et al (2023). There are many ways to approach roughness modelling for full scale ship simulations. This point was investigated in another aspect of the JoRes project, which is outside the scope of this paper, where extensive discussions and comparisons of different approaches to roughness modelling were conducted. Verification and validation procedures were performed on both the MV Regal cargo ship and a flat plate of comparable ship length. The Hutchins model was deemed acceptable and proved to be accurate in the case of the MV Regal cargo ship simulations in comparison to sea trial data. Extensive studies on the influence of roughness conversion on the flat plate were also conducted. After discussions with roughness experts and a review of the investigations, it is believed the Hutchins model is the most advanced one as of today as it considers the non-homogenous nature of hull roughness. The same process that was validated on the MV Regal was used to determine the roughness parameters for the tanker ship used in this blind benchmark study.

This workflow uses the Hutchins model to convert the AHR measurements to an equivalent sand grain roughness model that can be used with the roughness model proposed by Shultz (2007), where the non-dimensional U^+ is modified to adjust for roughness effects in the following manner:

$$U^+ = \frac{1}{\kappa}\log(y^+) + B - \Delta U^+ \quad (4)$$

Where κ is Karman constant and B is a constant.

The shift in ΔU^+ to account for the roughness is defined as:

$$\Delta U^+ = \begin{cases} 0 \rightarrow k^+ < 3 \\ \frac{1}{\kappa} ln(0.26k^+)^{sin}\left[\frac{\pi}{2}\frac{log(k^+/3)}{log(15)}\right] \rightarrow 3 < k^+ < 15 \\ \frac{1}{\kappa} ln(0.26k^+) \rightarrow 15 < k^+ \end{cases} \quad (5)$$

Where k^+ is defined as:

$$k^+ = \frac{kU_\tau}{\nu} \quad (6)$$

U_τ is the friction velocity, ν is the kinematic viscosity, and k is the applied sand grain roughness.

Since roughness was modeled, some modifications were made to the mesh in the vicinity of the hull compared to what Wheeler suggested (2021). Namely, the mesh size was set to be 6.25% of the base size. A target Y+ on the hull was set to 150 with 20 cells being used in the boundary layer mesh. In addition, the rudder was included and the size of the mesh in the vicinity of the rudder was set to 3.125% of the base size. The target Y+ on the rudder was set to 100 and 10 prism layer cells were used. The aspect ratio between the last layer of the boundary layer mesh and the volume mesh was between 1 and 2. The mesh used is shown below in Figure 4.

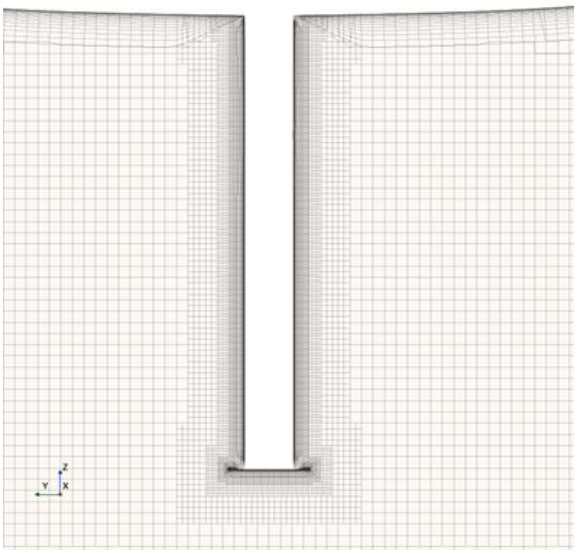

Figure 4: Section Slice of the computational mesh near the rudder and hull. Refinements made in the vicinity of the rudder and the boundary layer mesh applied to the hull can be seen.

The CFD model applied the Forced Moving Wave Tank (FMWT) approach, similar as to what is described by Wheeler et. al (2021), wherein the vessel starts in hydrostatic position and is accelerated to a target speed. In turn, the entire computational domain translates at this prescribed speed and volumetric boundary conditions employ wave forcing to enforce the inlet conditions. The interior of the domain solves the RANS equations. The applied inlet velocity assumes all components to be zero, representing flat, zero current conditions. This velocity is enforced at all sides of the domain, expect the top boundary where a hydrostatic pressure gradient is enforced in the domain. The reference, gauge pressure is set to 0 at the nominal free surface position. A forcing length of one vessel length and a forcing strength of 5 Hz are applied in the simulations. The reason for using this approach is it creates an intuitive framework that allows the same simulation file to be used in a maneuvering study (Which is not presented in this paper). An illustration of the boundary conditions and domain movement is highlighted below in Figure 5.

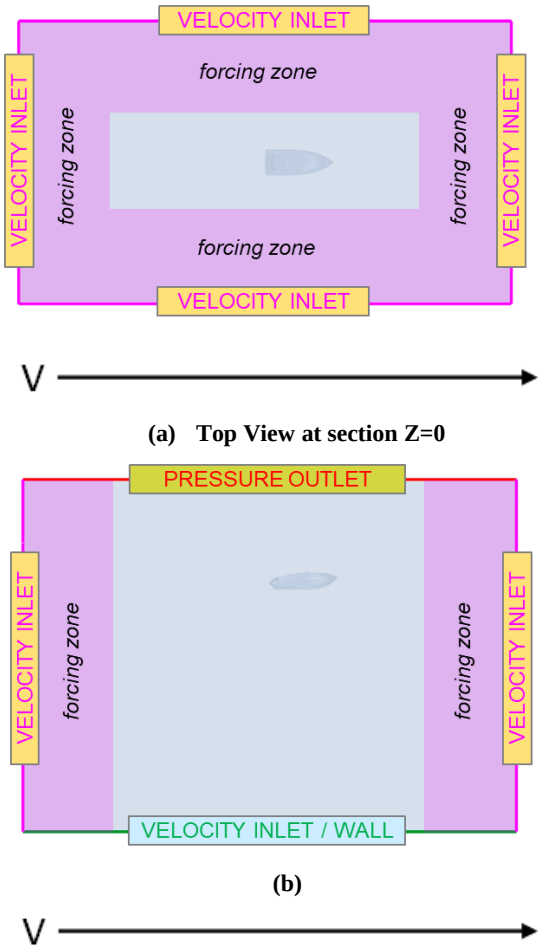

(a) Top View at section Z=0

(b)

(b) Side View at section Y=0

Figure 5: Representation of the boundary conditions applied in the FMWT approach. The entire domain moves with the vessel at its prescribed velocity V.

The vessel was free to heave and pitch while the forward velocity was prescribed. These motions were simulated using the dynamic fluid body interaction (DFBI) model available in Simcenter STAR-CCM+. This model will integrate the fluid traction loads on the body and solve the equations of motion for the vessel while also allowing for the inclusion of additional body forces. The use of an overset grid methodology was used to couple the moving vessel onto the FMWT domain. The overset domain is shown in Figure 6. Only the hull (with PIV unit attached), rudder, and propeller were modelled. Added resistance to account for bilge keels and the superstructure was simulated by including additional body forces to the vessel. The forces were determined based on ITTC procedures (2008). The drag on the bilge keels was approximated using Peck's formula (1976).

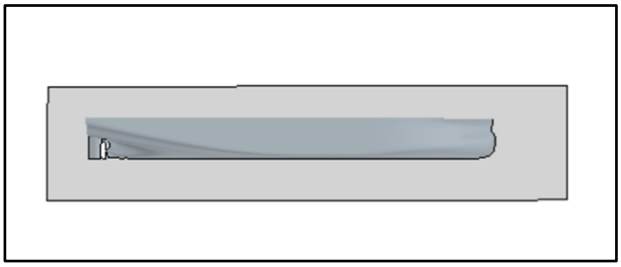

Figure 6: Hull surfaces used in the study and the rectangular overset grid used in this study.

The propulsion force was modeled by including the geometry of the propeller in the DFBI body and solving for the pressure and shear stresses on the propeller directly and integrating them across the surfaces to determine thrust forces. The fixed pitch propeller (FPP) with a propeller boss cap fin (PBCF) was modelled using a polyhedral grid and connected to the overset region via a topology-based sliding mesh interface as depicted in Figure 7. The base size of the mesh was set to the propeller diameter / 20. The mesh size on the propeller blades is 10% of the base size, with the leading and trailing edges set to be 0.5% of the base size. The maximum cell size allowed in the propeller region was set to 35% of the base size. The rotation rate of the propeller was prescribed and is superposed onto the vessel motion.

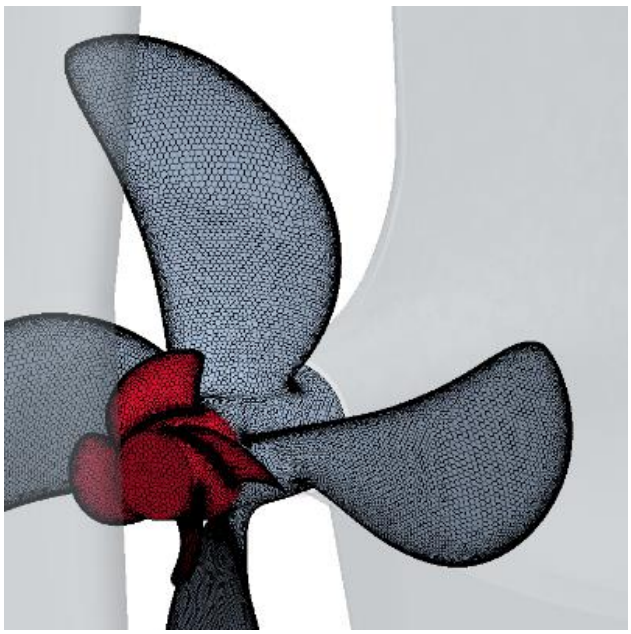

Figure 7: Computational grid of the propeller and propeller boss cap fin. Propeller (grey) and PBCF (red) with local computational grid shown.

The self-propulsion point was determined by building a linearized thrust coefficient controller in a similar manner as described by Nuutinen (2019). This algorithm is beneficial because it does not require any tuning parameters compared to a PID-based controller. The forward speed of the vessel is prescribed and the rotation rate to maintain the prescribed speed was adjusted until there was a suitable force balance within the ship-propeller system. The algorithm works in the following manner:

At any instant in time, the thrust coefficient, K_T, can be determined based on metrics available in the CFD simulation.

$$K_T = \frac{T}{\rho n^2 D^4} \tag{7}$$

Where T is the thrust of the propeller, ρ is the fluid density, n is the rotation rate, and D is the diameter of the propeller.

Then, if the thrust coefficient is assumed constant from one time interval to the another, then it follows:

$$T = \beta n^2 \tag{8}$$

And therefore β can be assumed to be constant to form an instantaneous, linearized derivative. Which implies:

$$\frac{dT}{dt} = 2\beta n \frac{dn}{dt} \tag{9}$$

Then, the change in thrust required to achieve a force balance is:

$$\frac{dT}{dt} = \frac{F_e}{\Delta t^*} \tag{10}$$

where F_e is the average error in the force balance of the ship-propeller system and Δt^* is an under-relaxation factor.

Then, imposing the thrust derivative, the change in rotation rate can be defined as:

$$\frac{dn}{dt} = \frac{F_e}{2\beta n \Delta t^*} \tag{11}$$

Since the CFD model is discretized in time, the derivative must also be discretized and the choice of the chosen time interval to determine the appropriate update in rotation rate is important to facilitate fast convergence. The time interval, Δt, used in these simulations was chosen to be the time for least one blade passing and for both the average F_e and T over one blade passing to be converged. By doing this, it promotes a faster convergence of the algorithm by looking at averaged force data that minimizes the influence of any local thrust oscillations coming from the propeller. Equation 11 can be rewritten in discretized form as:

$$n_t = n_{t-1} + \frac{F_e}{2\beta n_{t-1} \Delta t^*}(t_e - t_s) \tag{12}$$

Where n_t is the updated rotation rate, $n_{t-1}$is the previous rotation rate, t_s is the time when the propeller adjustment step starts and t_e is the time when the propeller adjustment step finishes and $\Delta t = t_e - t_s$.

The simulations were run in four stages. These stages are summarized as:

Stage 1: Set propeller rotation rate to 0. Run the simulation until the resistance of the ship, the trim, and the heave are converged. With the rotation rate set to 0, this allows for the use of a resistance-based time scale, where the time step used can be set as L/(200V). Where L is the length of the vessel and V is the prescribed speed ship. This is a fairly large time step, generally an order of magnitude larger than what is required for propeller modeling and will promote faster convergence as the generated waves and wake field will develop quickly.

Stage 2: Set the propeller to a guessed rotation rate. Any reasonable guess will work. Then run the simulation until the thrust of the propeller and the error function, F_e are converged. The time step used in this stage is set to one degree of propeller rotation per time step.

Stage 3: This stage finds the self-propulsion point by looping over the algorithm described in Equations 7 - 12 and adjusting the rotation rate of the propeller until F_e is balanced within 1% of the average hull resistance over the course of three propeller revolutions. In addition, the average thrust of the propeller, the average resistance of the hull, the heave, the pitch, the propeller rotation rate, and

the shaft power must all be suitably converged over 3 propeller revolutions until the algorithm stops iterating.

Stage 4: Once the self-propulsion point is found. The rotation rate is held constant, and the simulation is run for four complete propeller revolutions. During this stage, the average velocity over these four propeller revolutions is computed so the local velocity can be compared to the PIV measurements.

The entire process was embedded into the Simcenter STAR-CCM+ simulation file to create a parameter-based, script-free template. Different loading conditions and speeds can be investigated with the same simulation file with a simple parameter change. As such, the file was run at both 11.25 knots and 13.34 knots. The mesh for the tanker consisted of 37.3 million cells and the simulations were run on 192 CPUs. The run time was about 100 hours for the simulations.

The JoRes project policy suggests that hard data describing the performance of the vessel shall not be shared publicly until the end of 2024. Nevertheless, typical convergence plots are shown below. In Figure 8, the running average of the force balance, normalized by the final hull resistance, and averaged over 3 propeller revolutions is plotted and the 4 stages are overlayed on top of the graph. The first stage requires about 16% of the total simulation time and the self-propulsion algorithm requires about 45%. Calculating the PIV data requires about 12% of the simulation time. In addition, a plot of the normalized engine power is plotted as well, and it can be seen how the averaged power converges vs the instantaneous power prediction. The instantaneous power oscillates with the blade passing frequency primarily due to oscillations in the propeller torque. Operating on the averaged shaft power will lead to fast, stable convergence.

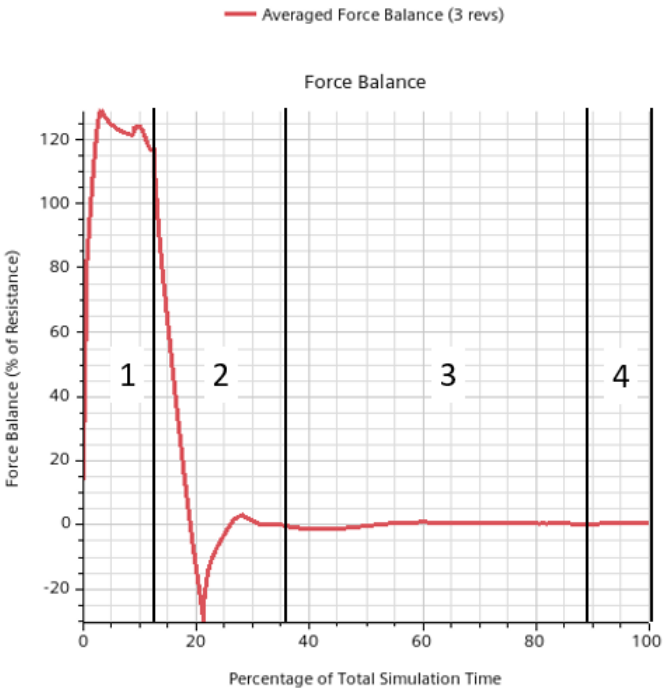

(a) Typical convergence for the Force balance in the ship-propeller system.

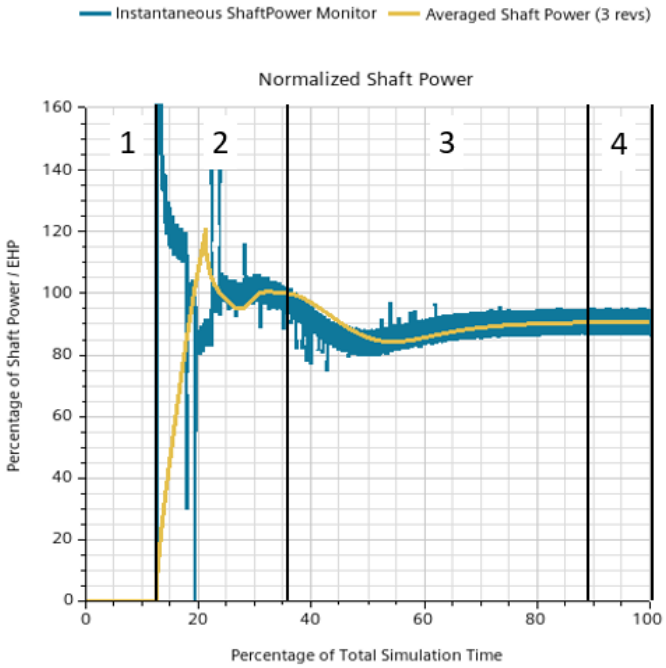

(b) Normalized Engine Power plotted vs Time Step

Figure 8: Typical convergence. (a) The force balance, normalized by the resistance of the hull at the final time step, is shown across the 4 stages of the simulation. (b) The normalized shaft power, both instantaneous and averaged is shown across the 4 stages of the simulation.

5 COMPARISONS OF CFD RESULTS TO SEA TRIAL MEASUREMENTS

Table 1: Comparison of results between the CFD model and Sea Trial Measurements.

Percent Comparison of CFD Results to Sea Trial Measurements		
Metric	11.25 knots	13.34 knots
Propeller Rotation Rate	0.29%	0.66%
Torque	-5.75%	-4.64%
Shaft Power	-5.43%	-3.69%

The key metrics in a self-propulsion test and simulation are deriving the propulsive powering metrics to size the engine power plant and shaft of the propeller. Overall, the simulations matched the sea trial favorably and a summary of the results is shown in Table 1. Positive values in the table indicate over-prediction of CFD results compared to sea trial data and negative values suggest the CFD simulations underpredict the metrics compared to sea trial data. It should be noted that the results presented at SMP2015 had also good correlation with experimental values however there were a few significant points: 1. Ship scale SMP2015 results were not postprocessed according to the ISO15016 standard, so uncertainty level was significantly higher. 2. Hull and propeller roughness was not measured in 2015 and a few assumptions were made to estimate those values. Moreover, the model of conversion of the Average Hull Roughness into the Equivalent Sand Grain roughness proposed by Hitchins (2023) was not available in 2015.

As mentioned, the uncertainty metrics in the power estimation for the sea trial tests are on the order of 4% – 6%. Therefore, the results can be said to be validated as the CFD results are within this range.

Possible ways to improve the simulations would be to explicitly model the bilge keels and superstructure. Overall, the simulation results match quite well.

In addition to determining the required shaft power, the JoRes1 Tanker vessel was equipped with a Flow Pike PIV measuring unit to measure the averaged velocities at the section in front of the propeller during the sea trial. As such, a comparison of the flow field in the CFD to the sea trial measurement is of high interest. A comparison of the PIV measurements is shown in Figures 9 and 10. The results between the two speeds are mostly similar.

The measurements match very well in areas of low flow gradients. In areas where there are high gradients, the results seem to differ much more. One such reason is the spatial resolution in the CFD simulations is about 25 times larger than the reported spatial resolution of the PIV measurements. Further refining the computational grid in the CFD model would likely resolve these gradients more accurately.

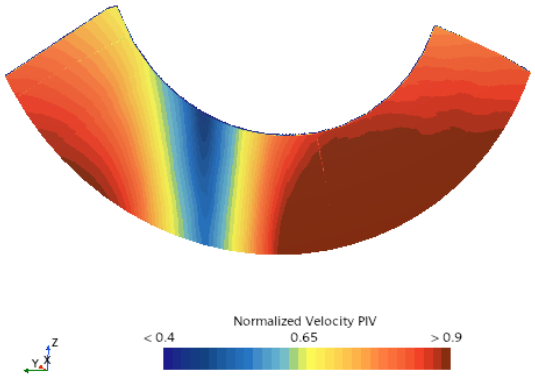

(a) Velocity field determined via PIV measurements during sea trial.

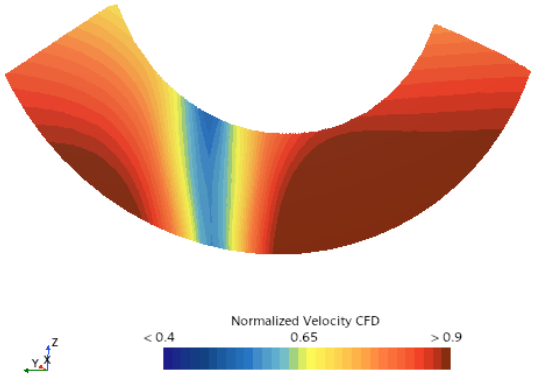

(b) Velocity field determined in the CFD calculation.

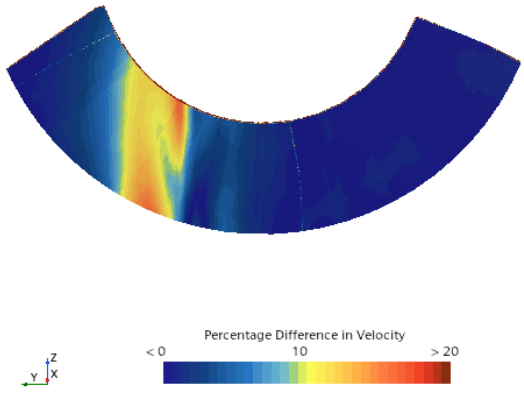

(c) The PIV measurements are compared locally to the CFD results.

Figure 9: Velocity results from the 13.34 knots case. (a) Velocity measurements from PIV data. (b) Velocity calculations from CFD simulation. (c) Plots the percentage difference in velocity of PIV data compared to CFD data.

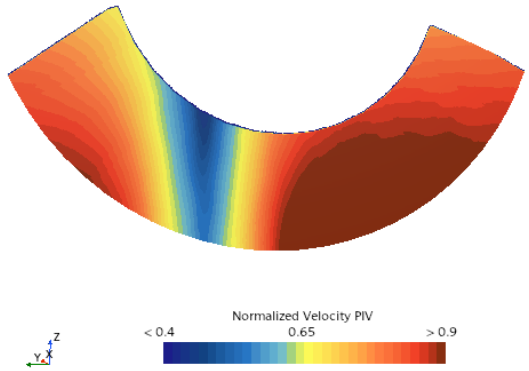

(a) Velocity field determined via PIV measurements during sea trial.

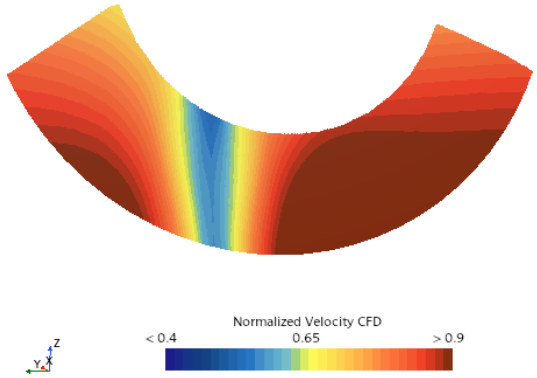

(b) Velocity field determined in the CFD calculation.

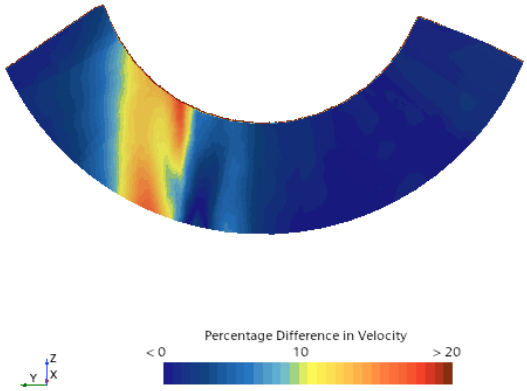

(c) The PIV measurements are compared locally to the CFD results.

Figure 10 Velocity results from the 11.25 knots case. (a) Velocity measurements from PIV data. (b) Velocity calculations from CFD simulation. (c) Plots the percentage difference in velocity of PIV data compared to CFD data.

6 CONCLUSIONS

Comparing this paper with the one published at SMP'2015 (Ponkratov and Zegos 2015) for a similar size tanker it can be concluded that there is significant development in the maritime industry about ship-scale CFD simulations and their validations. The methods are generally matured and the computational time for multi-million cells mesh becomes practical and realistic. Ship scale validation cases become available within global joint research projects (like JoRes) and individually. The cases are not limited to standard speed and power curves but also offer comprehensive datasets, for example propeller flow measured by a newly introduced ship scale PIV method. Noticeable research has been performed to measure hull roughness on actual vessels, develop a methodology to convert the measured Average Hull Roughness into CFD readable, equivalent Sand Grain roughness and implement the new roughness functions in CFD. All of this contributes to a better understanding of ship efficiency potential and ultimately to the designing of future zero-emission vessels. It would be interesting to see how ship scale simulation will evolve in the next ten years. It is believed the main change will be in the computational time allowing to perform such calculations within minutes.

REFERENCES

Birvalski, M., Struijk, G. D., Ponkratov, D. (2023). Full-scale PIV measurements of the propeller inflow, 15th International Symposium on Particle Image Velocimetry – ISPIV 2023, June 19–21, San Diego, California, USA

DNV (2023). MARITIME FORECAST TO 2050, Energy Transition Outlook, September 2023.

Hitchins, N., Ganapathisubramani, B., Schultz, M., Pullin, D., (2023). Defining an equivalent homogeneous roughness length for turbulent boundary layers developing over patchy or heterogeneous surfaces, Ocean Engineering, 271, 113454.

IMO (2023). Strategy on Reduction of GHG Emissions From Ships, Resolution, MEPC.377(80), adopted on 7 July 2023.

ITTC. Recommended Procedures and Guidelines, Performance, Propulsion 1978 ITTC Performance prediction method, 2008.

Mikkelsen, H., Steffensen, M. L. (2016). 'Full-scale validation of CFD model of a self-propelled ship', Master thesis, Technical University of Denmark.

Mikulec, M., & Piehl, H., (2023). 'Verification and validation of CFD simulations with full-scale ship speed/power trial data', Brodogradnja/Shipbuilding, Volume 74 Number 1, http://dx.doi.org/10.21278/brod74103

Niklas, K., Pruszko, H. (2019). 'Full-scale CFD simulations for the determination of ship resistance as a rational, alternative method to towing tank experiments', Ocean Engineering 190 (2019).

Nuutinen, M., (2019). 'Automated self-propulsion point search algorithm for ship performance CFD simulations', Sixth International Symposium on Marine Propulsors, SMP'19 Rome, Italy.

Orych, M., Werner, S., Larsson, L. (2021). 'Validation of full-scale delivered power CFD simulations', Ocean Engineering 238

Peck, R.W., (1976). 'The determination of appendage resistance of surface ships', AEW Technical Memorandum, 76020.

Ponkratov, D., Zegos, C., (2014). 'Ship scale CFD self-propulsion simulation and its direct comparison with sea trial results'. the International Conference on Computational and Experimental Marine Hydrodynamics. MARHY'14, Chennai, India.

Ponkratov, D., Zegos, C. (2015). 'Validation of Ship Scale CFD Self-Propulsion Simulation by the Direct Comparison with Sea Trials Results'. Fourth International Symposium on Marine Propulsors, Austin, TX, USA, 31 May–4 June.

Ponkratov, D., (2017). 'Workshop on ship scale hydrodynamic computer simulations'. Proceedings: Lloyd's Register's Full-Scale Numerical Modelling Workshop.

Ponkratov, D., Struijk, G., Birvalski, M., Elbertsen, M.,(2022). 'A journey to unique PIV flow measurements at ship scale', 7th Hull Performance and Insight conference HullPIC2022, Tullamore, Ireland, May.

Ponkratov, D., Struijk, G., (2023). 'Quantifying the Uncertainty of High-Fidelity Speed/Power Trials', 8th Hull Performance and Insight conference HullPIC2023, Pontignano, Italy, 28-30 August.

Ponkratov, D., (2023). 'JoRes Joint Research Project - the largest global community developing a benchmark for ship scale CFD', 25th Numerical Towing Tank Symposium, Portugal, 15-17 October.

Schultz, M., (2007). 'Effects of coating roughness and biofouling on ship resistance and powering', Biofouling 23.5 (2007): 331-341.

Schultz, M., and Hutchins, N., (2021). Prediction of an effective hydraulic length scale for surfaces with heterogeneous roughness, APS-DFD, 74th Annual Meeting, Phoenix, AZ.

Sun, W., Hu, Q., Hu, S., Su, J., Xu, J., Wei, J. and Huang, G. (2020). 'Numerical Analysis of Full-Scale Ship Self-Propulsion Performance with Direct Comparison to Statistical Sea Trail Results', J. Mar. Sci. Eng., 8, 24; doi:10.3390/jmse8010024

Wheeler, M., (2021). 'Speeding up Hydrodynamic Simulations with a Parametric Templated Approach', SNAME Maritime Convention. SNAME.

Wheeler, M., et al. (2021). 'Using VOF Slip Velocity to Improve Productivity of Planing Hull CFD Simulations', SNAME International Conference on Fast Sea Transportation.